

## Continuum protons from $^{58}\text{Ni}(p, p')$ at incident energies between 100 and 200 MeV

S. V. Förtsch, A. A. Cowley, J. J. Lawrie, D. M. Whittal, J. V. Pilcher, and F. D. Smit

*National Accelerator Centre, Faure, 7131, South Africa*

(Received 29 October 1990)

The inclusive reaction  $^{58}\text{Ni}(p, p')$  was studied at incident energies of 100, 120, 150, 175, and 200 MeV for scattering angles between  $15^\circ$  and  $120^\circ$ . Angular distributions at various emission energies are analyzed in terms of a quasifree knockout reaction mechanism, combined with parametrized systematics which should represent multistep contributions. Reasonable agreement between the experimental data and calculated distributions is obtained, with a consistent incident-energy dependence. The proportion of the quasifree component amounts to  $\sim 30\%$  of the preequilibrium yield. The quasifree contribution appears to be in agreement with the first-step yield of the statistical multistep-direct emission theory.

### I. INTRODUCTION

The preequilibrium reaction process as manifested in nucleon-nucleus inclusive scattering has been of theoretical and experimental interest for many years.<sup>1,2</sup> Most of the theoretical models<sup>2</sup> treat the reaction mechanism in terms of a succession of nucleon-nucleon collisions with particles emitted from the various stages as the projectile energy is progressively dissipated in the target nucleus. Another feature which these models have in common is that they all predict emission from the first step to be predominant. This, in turn, motivates investigations into the extent to which preequilibrium reactions can be viewed as proceeding through a quasifree nucleon-knockout reaction mechanism<sup>3-5</sup> only.

It is generally believed<sup>6-8</sup> that a quasifree knockout mechanism should manifest itself in preequilibrium energy spectra as peaks with the characteristic kinematic features of a collision between a projectile (nucleon) with a bound target nucleon. Whereas such quasifree peaks are observed very clearly<sup>9</sup> at incident energies of several hundred MeV, the situation at 100–200 MeV is more obscure. For example, Wu *et al.*<sup>10</sup> find a small peak in the continuum energy spectra for  $^{58}\text{Ni}(p, p')$  at 90 and 100 MeV, which appears to be consistent with quasifree scattering. However, at 150 MeV incident energy for the same reaction,<sup>8</sup> where a clearer signature of quasifree scattering would be expected, the dramatic absence of any such feature is encountered. Experimental difficulties have been blamed<sup>11</sup> for some discrepancies which have been observed. As it is well known<sup>12,13</sup> that the measurement of preequilibrium spectra requires careful attention to projectile beam properties and other experimental conditions, it is tempting to attribute many of the inconsistencies to experimental systematic error. As pointed out by Kalbach,<sup>14</sup> in the absence of duplicate data from different laboratories, the reliability of experimental data has to be judged solely on the observed systematic trends.

Recent extreme views on the importance of quasifree scattering in the incident-energy range of interest in the present study are represented by those of Smith and Bozoián<sup>5</sup> and Kalbach.<sup>15</sup> Whereas the former authors cal-

culate the proportion of quasifree scattering in  $(p, p')$  at 90 MeV as ranging from  $\sim 70\%$  for the target nucleus  $^{27}\text{Al}$  to  $\sim 45\%$  for  $^{209}\text{Bi}$ , Kalbach estimates the contribution from this mechanism to be negligible below a threshold of 150 to 200 MeV. Although Kalbach alludes to a difference of terminology in these two investigations, it is nevertheless not obvious that the results of these studies should differ as much as they do.

In previous work we have found that the shape of preequilibrium spectra of  $^{12}\text{C}(p, p')$  over a wide angular range at incident energies of 90 and 200 MeV can be accounted<sup>16</sup> for by the simplistic assumption that only quasifree knockout occurs. In a further study<sup>17</sup> on  $^{197}\text{Au}(p, p')$  between incident energies of 100 and 200 MeV, a small but significant quasifree contribution is inferred, and a subsequent coincidence experiment on  $^{197}\text{Au}(p, p'p'')$  at 200 MeV (Ref. 18) corroborates this conclusion. The qualitative presence or absence of clear "quasifree" peaks in preequilibrium spectra may not always be a definitive criterion for judging the magnitude of the contribution traceable to a knockout mechanism. For example, it was concluded<sup>19</sup> for  $^4\text{He}(p, p')$  at 100 MeV that  $\sim 70\%$  of the inclusive continuum yield is attributable to such a mechanism, in spite of the fact that the observed spectrum is quite featureless as a result of cluster knockout contributions.

The present study presents new preequilibrium data on the inclusive reaction  $^{58}\text{Ni}(p, p')$  at incident energies of 100–200 MeV. An effort is made to evaluate the experimental reliability of all the present data implicitly by comparing some spectra with the few existing measurements. The experimental data are analyzed in terms of a background (of as yet unspecified origin) as was inferred from Kalbach's<sup>14</sup> phenomenology applied<sup>17</sup> to  $^{197}\text{Au}(p, p')$  in the same range of incident energy, to which a nucleon-knockout component is added incoherently. The quasifree knockout component from representative valence shells is treated in the distorted-wave impulse approximation<sup>20</sup> (DWIA) as in Refs. 16, 19, and 21.

In Sec. II, experimental details are described, and in Sec. III some of our experimental data are compared with

previously published results which were obtained at other laboratories. The quasifree knockout model and the parametrized multistep formalism, which are combined incoherently, are summarized in Sec. IV. In Sec. V the experimental and theoretical results are compared and discussed. Finally, conclusions are presented in Sec. VI.

## II. EXPERIMENTAL PROCEDURE

The experiment was performed at the cyclotron facility of the National Accelerator Centre. A detailed description of the equipment and the layout is given in Ref. 22 and references therein. The experimental procedure was essentially the same as for the measurements described in Ref. 17.

Continuum spectra for the inclusive reaction  $^{58}\text{Ni}(p,p')$  were measured at incident laboratory beam energies of 100, 120, 150, 175, and 200 MeV in an angular range from  $15^\circ$  to  $120^\circ$ . The uncertainty in absolute beam energy was deduced from the operating conditions of the cyclotron to be less than 0.5 MeV. The target was a self-supporting nickel foil enriched to 98% in  $^{58}\text{Ni}$  with a thickness of  $(1.10 \pm 0.08)$  mg/cm<sup>2</sup> and uniformity of better than 2%/mm.

The detector telescope consisted of a 1000  $\mu\text{m}$  Si ( $\Delta E$ ) detector, followed by a  $75 \times 125$  mm NaI(Tl) stop detector ( $E$ ). An active collimator, as described in Ref. 16, was used to define a solid angle of 0.9 msr and an angular acceptance of  $2^\circ$ .

Energy calibration of the silicon detector was performed with  $\alpha$  particles from a  $^{228}\text{Th}$  source. The kinematics for the elastic scattering of protons from carbon and hydrogen in a thin plastic ( $\text{CH}_2$ ) target was used to determine the slightly nonlinear energy calibration of the NaI detector. Forward-angle elastic scattering from a carbon target, on both sides of the beam, was used to determine the angular offset of the beam direction to better than  $0.2^\circ$ . The beam spot of less than 3 mm in diameter remained centered on the target to better than 0.5 mm.

Beam halo, which might affect measurements at forward angles, was monitored frequently by comparing the count rate from an empty target frame with that of the rate from the  $^{58}\text{Ni}$  target. Contributions due to background were always less than 5% (typically 0.5% to 1%) and were corrected for as deemed necessary.

Standard electronics together with an on-line computer system were used to write event-by-event data to tape for subsequent off-line analysis. A light-emitting diode (LED) pulser system allowed for corrections to be made for possible gain drifts in the photomultiplier tube of the NaI detector. The LED was triggered at a rate proportional to the beam current and these pulses, which were also recorded, were used to correct for electronic dead time.

The correction for the NaI detector efficiency was based on the procedure described in Ref. 23. The extent of the particle identification gate in the  $\Delta E$  vs  $E$  spectrum, which selected protons, was taken into account in

the efficiency correction. The cross sections are believed to be accurate to within a systematic error of 10%.

## III. COMPARISON WITH PUBLISHED SPECTRA

In order to substantiate the accuracy to be associated with our experimental procedure, selected  $^{58}\text{Ni}(p,p')$  continuum spectra at 100 and 150 MeV are compared in Fig. 1 with published data at the same incident energies. This comparison also serves to confirm the qualitative features of the results for  $^{58}\text{Ni}(p,p')$  at 100 and 150 MeV, as was documented previously.<sup>10,8</sup>

Our new data for the two sets of incident energies and angles are in reasonable (within  $\sim 10\%$ ) shape agreement with existing<sup>8,10,13</sup> data, as shown in Fig. 1. However, a discrepancy of 20–30% in absolute magnitude between our data and those of Wu *et al.*<sup>10</sup> and Segel *et al.*<sup>8</sup> is observed. While these differences correspond roughly to those that should be expected for the maximum combined uncertainties (20% and 25%, respectively), they are not unreasonably large. It should be noted that in other comparisons which we have made with continuum spectra which were measured elsewhere, generally much better agreement in absolute magnitude was obtained (see, e.g., Ref. 16).

Clearly, our measurements qualitatively confirm the conclusion of Segel *et al.*<sup>8</sup> that no prominent quasifree peak is discernible at an incident energy of 150 MeV. Although internal consistency checks confirmed the estimated systematic error of our work to be within 10%, the comparisons in this section do not rule out the possible need for readjustment of our absolute cross section scale by  $\sim 20\%$ . However, should this be necessary, the results and conclusions of Secs. V and VI would not be affected, except for a trivial rescaling.

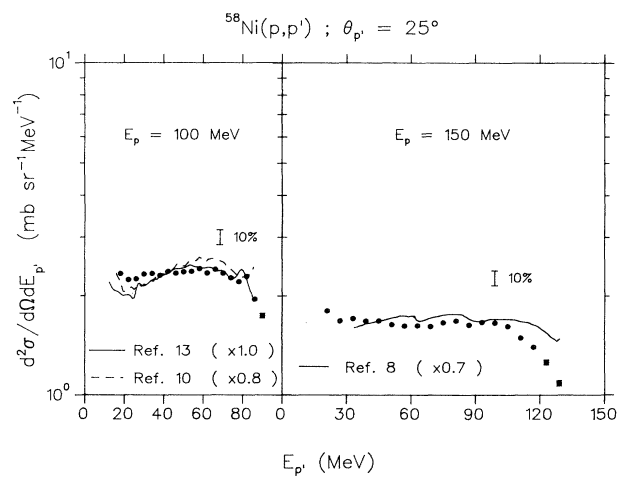


FIG. 1. Experimental continuum energy spectra obtained in this work ( $\bullet$ ) for  $^{58}\text{Ni}(p,p')$  at a scattering angle of  $25^\circ$ , compared with published measured results of Segel *et al.* (Ref. 8), Wu *et al.* (Ref. 10), and Cowley *et al.* (Ref. 13), which are shown as curves.

#### IV. THEORETICAL MODEL

The double differential cross section for the inclusive reaction  $^{58}\text{Ni}(p,p')$  is expressed as an incoherent sum of a quasifree (QF) knockout term and a cross section which represents the contribution from multiple scattering (MS). The expression

$$\frac{d^2\sigma}{d\Omega dE_{p'}} = \frac{d^2\sigma_{\text{QF}}}{d\Omega dE_{p'}} + \frac{d^2\sigma_{\text{MS}}}{d\Omega dE_{p'}} \quad (1)$$

is then in conceptual agreement with the statistical multistep-direct emission model of Feshbach, Kerman, and Koonin<sup>24</sup> if the knockout term  $d^2\sigma_{\text{QF}}/d\Omega dE_{p'}$  is identified with first-step emission and  $d^2\sigma_{\text{MS}}/d\Omega dE_{p'}$  is taken to include the subsequent steps. Equation (1) is also the basic expression of Smith and Bozian<sup>5</sup> and Chiang and Hüfner,<sup>4</sup> and whereas our treatment of the QF term differs only in the details of the calculation from that of Refs. 4 and 5, we prefer to use a phenomenological approach to the MS part, as discussed below.

##### A. Quasifree scattering

The distorted-wave impulse approximation (DWIA) model<sup>20</sup> was used to calculate the QF component of the cross section. In this model the cross section for a reaction  $A(a,a'b)B$  can be written as<sup>20</sup>

$$\frac{d^3\sigma}{d\Omega_a d\Omega_b dE_{a'}} = S_L K \frac{d\sigma}{d\Omega_{a-b}} \sum_{\lambda} |T_L^{\lambda}|^2, \quad (2)$$

where  $S_L$  is the spectroscopic factor for the final state in  $B$ ,  $K$  is a kinematic factor, and  $d\sigma/d\Omega_{a-b}$  is a half-shell two-body cross section for  $a-b$  scattering. The quantity  $\sum |T_L^{\lambda}|^2$  is a distorted momentum distribution for a particle  $b$  bound in the target  $A$  with angular momentum  $L$  (projection  $\lambda$ ).

In this application of the model it is assumed that particle  $a'$  is detected after a quasifree collision with particle  $b$  which remains undetected. Calculations were performed with the code<sup>25</sup> THREEDD. A Woods-Saxon well with a radius parameter of 1.25 fm and a diffuseness of 0.65 fm was used<sup>26</sup> to generate the nucleon bound orbitals of the  $^{58}\text{Ni}$  target. Energy-dependent optical-potential parameters of Nadasen *et al.*<sup>27</sup> were used to calculate distorted waves for the proton  $a$  and nucleons  $a'$ , and as discussed by Whittall *et al.*,<sup>19</sup> a purely real potential was used for the undetected particle. Both the  $pp$  and  $pn$  scattering processes were approximated by the on-shell value of  $d\sigma/d\Omega_{a-b}$  evaluated at either<sup>28,29</sup> the final or initial proton-nucleon relative energy and angle (final-energy and initial-energy prescription, respectively). Spin-orbit effects,<sup>30</sup> the effective polarization<sup>31</sup> of the struck nucleon, and nonlocality<sup>32</sup> were ignored for calculational convenience, but this is not expected to alter the results significantly. Other details of the calculation are similar to those of Ref. 21.

The cross section for the detected particle  $a'$  is obtained by integration over the solid angle of the unobserved nucleon  $b$ , which gives

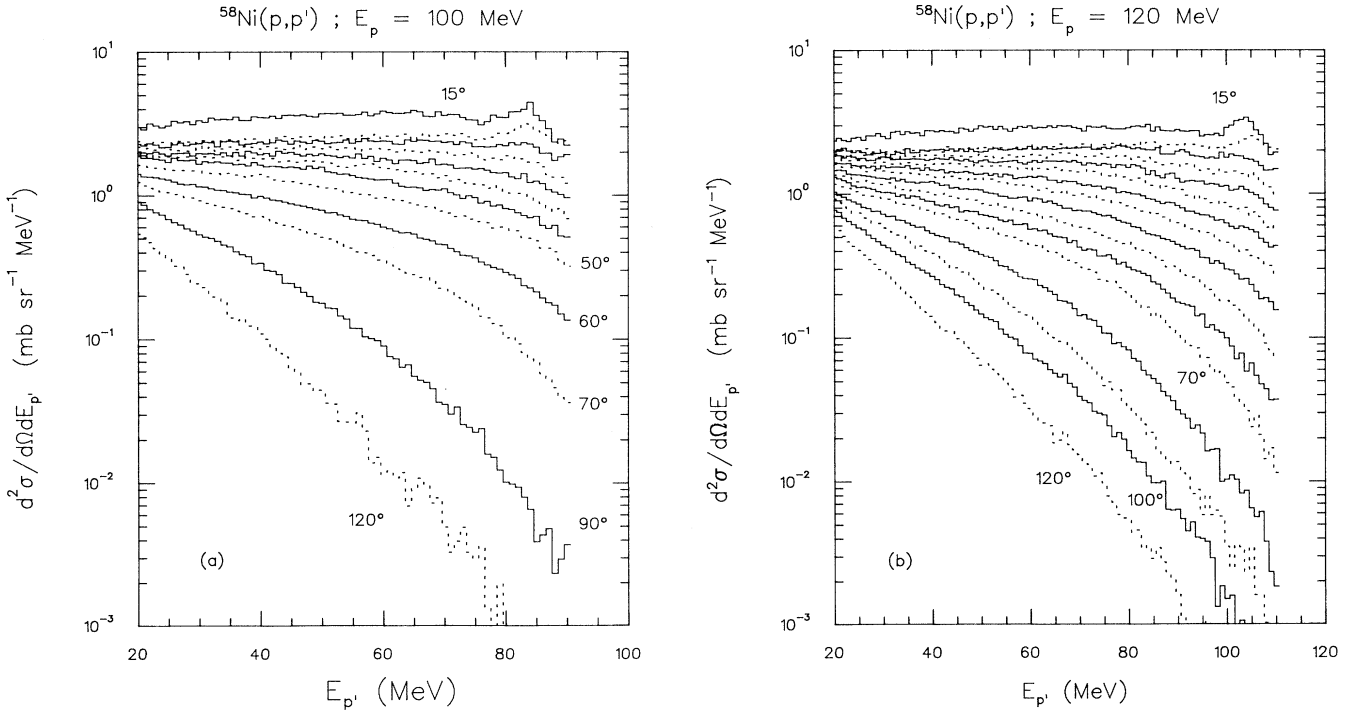


FIG. 2. Laboratory differential energy spectra for  $^{58}\text{Ni}(p,p')$  as a function of emission energy  $E_{p'}$  at various incident energies  $E_p$ . Spectra are shown in  $5^\circ$  steps up to the second angle indicated, and in  $10^\circ$  steps thereafter. Data in the energy range corresponding to elastic and inelastic excitation of discrete states in  $^{58}\text{Ni}$  are not shown. Some spectra have been multiplied by the indicated factors for clarity of display.

$$\frac{d^2\sigma}{d\Omega_a dE_{a'}} = \int \frac{d^3\sigma}{d\Omega_a d\Omega_b dE_{a'}} d\Omega_b. \quad (3)$$

The calculation is relatively insensitive to the details of the shells. Proton-knockout contributions from the

valence proton states of major yield ( $1f_{7/2}$ ,  $2s_{1/2}$ , and  $1d_{3/2}$ ) were summed incoherently with relative spectroscopic factors taken from Reiner *et al.*<sup>33</sup> A related occupation probability was used as a spectroscopic factor for the neutron  $1f_{7/2}$  state which should contribute most of the yield from neutron knockout.

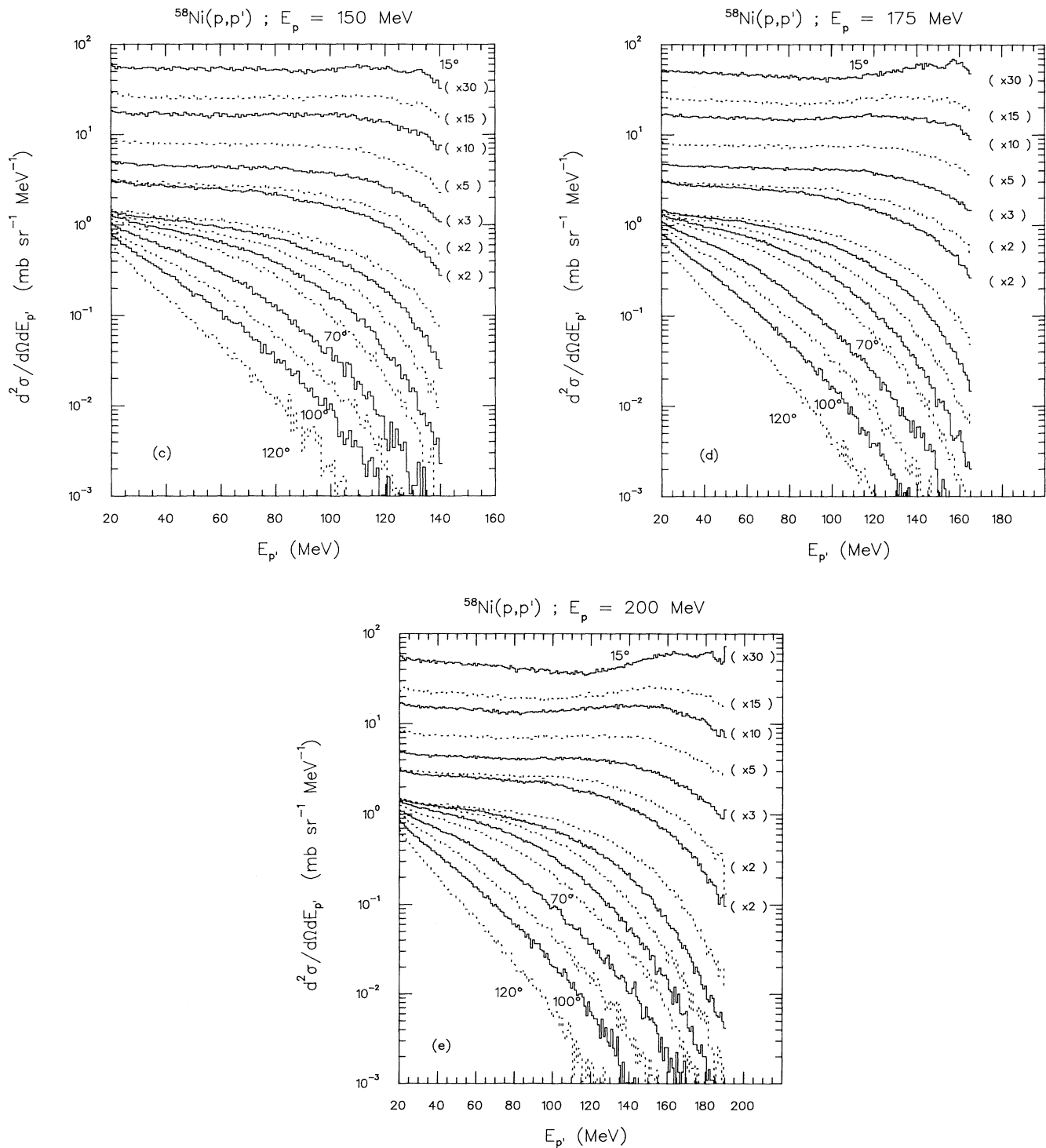


FIG. 2. (Continued).

### B. Phenomenological parametrization of multistep contributions

Instead of using available semiclassical or quantum mechanical theories to model the multistep contributions, we have based the calculation on the phenomenological parametrization of Kalbach.<sup>14</sup> The main reason for this is that doubts exist<sup>34</sup> as to the ability of semiclassical models such as the hybrid model to describe angular distributions in the incident-energy region above 100 MeV. This concern extends also to the individual components of the scattering chain. Also, despite the recent progress which has been made with quantum mechanical models in reproducing  $(p,n)$  and  $(p,p')$  data up to 160 MeV (Refs. 34 and 35) for certain target nuclei, the reliability of the calculations still needs to be demonstrated at higher incident energies and for a larger mass range.

It is postulated that the phenomenological expression of Kalbach<sup>14</sup> for continuum angular distributions, with the minor modification of the prescription as required for  $^{197}\text{Au}(p,p')$  at 120–175 MeV (Ref. 17), is a useful description of the multistep component. This expectation follows from the way in which the parametrization was de-

rived,<sup>14</sup> and also from its ability to reproduce angular distributions at large angles for the scattering of protons from a heavy target<sup>17</sup> at an incident energy of 100–120 MeV, for which multiple scattering should dominate.

For a purely direct reaction, which should be the dominant component of our data, the cross section for continuum angular distributions is given<sup>14</sup> by

$$\frac{d^2\sigma}{d\Omega dE_{p'}} = \sigma_D \frac{\eta}{\sinh\eta} \exp(\eta \cos\theta), \quad (4)$$

where  $\theta$  is the center-of-mass scattering angle. The quantity  $\sigma_D$  is a normalization factor obtainable either through experiment or from other theories, and is related to the angle-integrated yield  $d\sigma/dE_{p'}$ . In this work the value of  $\sigma_D$  is found by normalizing to the large-angle data. The slope  $\eta$  is expressed as

$$\eta(e_p, e_{p'}) = 0.04EX + 1.8 \times 10^{-6}E^3X^3 + 1.9X^4,$$

with

$$X = e_{p'}/e_p,$$

$$e_{p'} = E_{p'} + S_p,$$

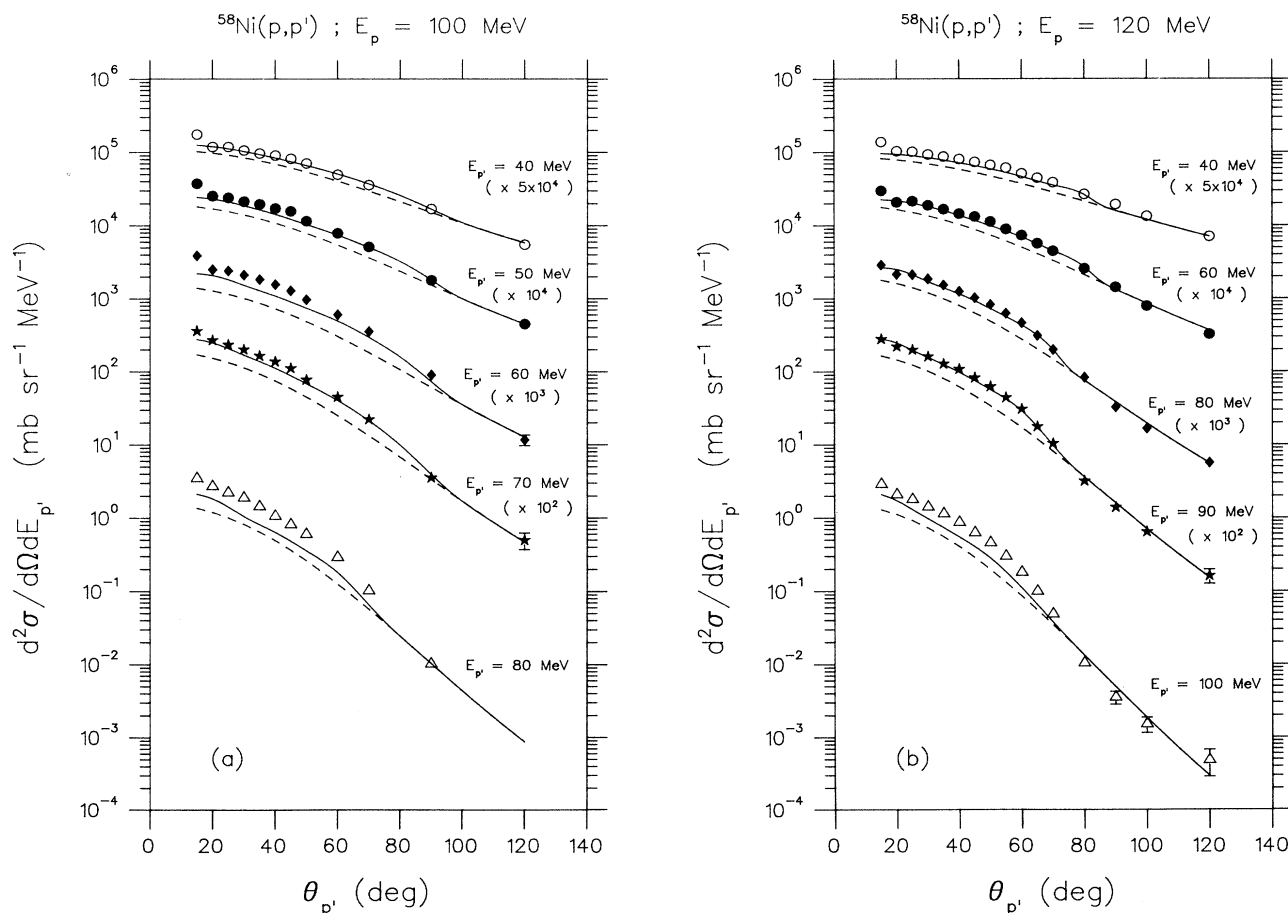


FIG. 3. Angular distributions for  $^{58}\text{Ni}(p,p')$  at various incident energies  $E_p$  and emission energies  $E_{p'}$ . Statistical error bars are shown where these exceed the symbol size. The parametrized yield which is assumed to represent a multiple-scattering contribution is shown as a dashed curve, and the incoherent sum with a quasifree component is indicated by a continuous curve. Results are multiplied by the factors as indicated for display, and are given in the laboratory coordinate system.

and

$$e_p = E_p + S_p.$$

The quantity  $S_p$  is the separation energy as given by Kalbach<sup>14</sup> while  $E_p$  and  $E_{p'}$  are the incident and emission energies, respectively. The value of the parameter  $E$  is adopted from a study<sup>17</sup> of  $^{197}\text{Au}(p,p')$  at incident energies between 100 and 200 MeV—a procedure which has also been demonstrated<sup>35</sup> to give better agreement with  $^{90}\text{Zr}(p,p')$  data at 120 MeV than the original<sup>14</sup> parametrization. It should be noted that at incident energies of 100 and 200 MeV the modified parametrization coincides with the original version, and between these energies a more realistic incident-energy dependence of  $\eta$  is obtained.

### V. RESULTS AND DISCUSSION

Laboratory differential energy spectra for the inclusive reaction  $^{58}\text{Ni}(p,p')$  at various incident energies are shown in Fig. 2. Corresponding angular distributions at various ejectile energies are displayed in Fig. 3.

The continuum spectra in Fig. 2 all reveal a general trend of exponential falloff at large scattering angles, and at the forward angles the spectra are rather featureless. As has been mentioned, the spectra are in general agreement with previous measurements of Cowley *et al.*<sup>13</sup> and Wu *et al.*<sup>10</sup> at 100 MeV and by Segel *et al.*<sup>8</sup> at 150 MeV at angles where these measurements can be directly compared with our spectra.

It should be noted that the large drop in cross section in the continuum energy spectra between the scattering angles of  $15^\circ$  and  $20^\circ$  at incident energies of 100 and 120 MeV may only be an artifact of a much larger systematic uncertainty at the smaller angle than the estimated 10% for the rest of the data. This comes mainly from the uncertainty of the detector-efficiency correction introduced by a dominant peak of elastically scattered protons at very forward angles at these energies. This phenomenon increases the uncertainty in the correction procedure of reducing counts in lower energy bins in order to account for reaction losses in the higher energy bins. At  $20^\circ$  and beyond, this specific problem is less severe.

Calculations of the quasifree knockout component

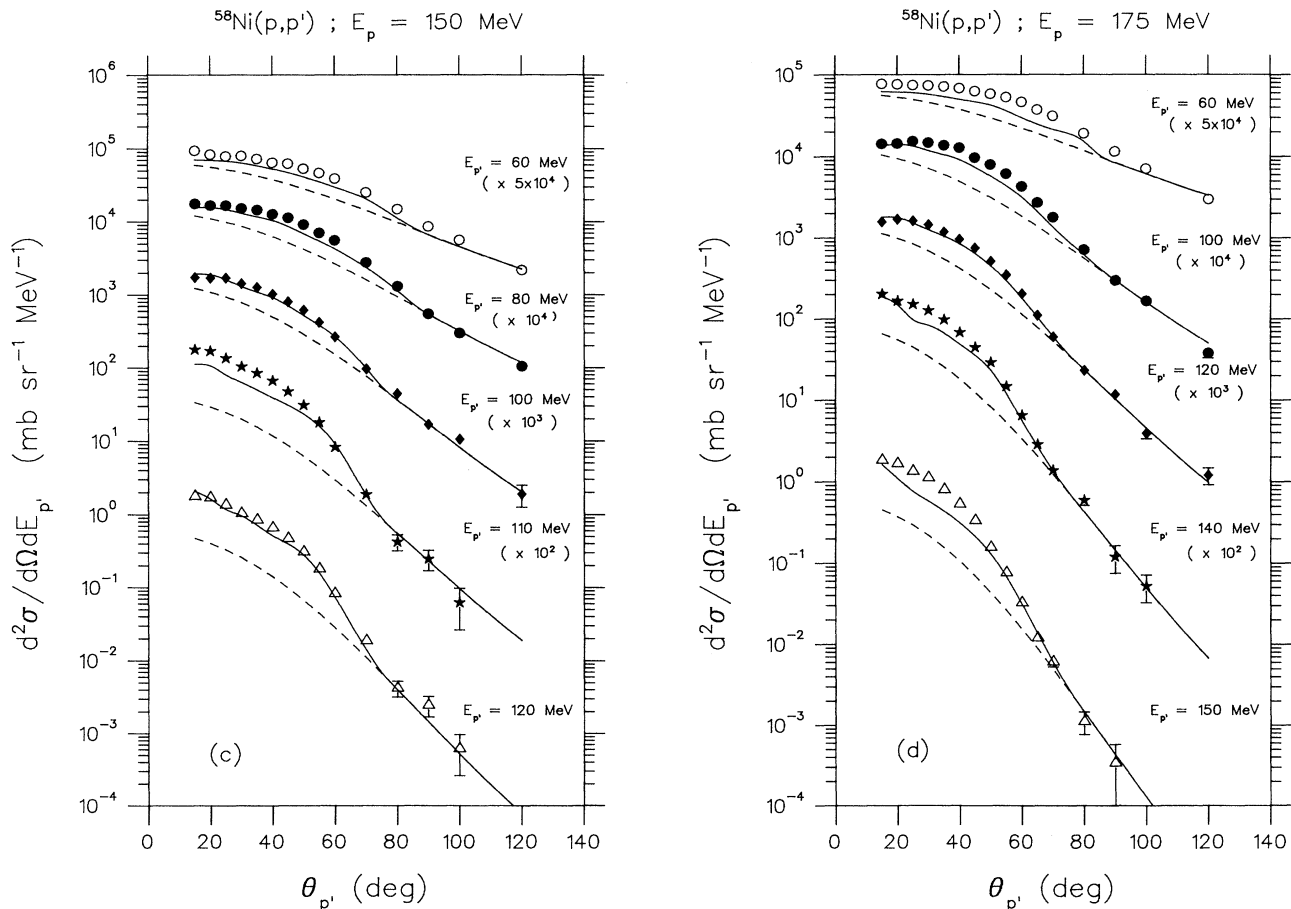


FIG. 3. (Continued).

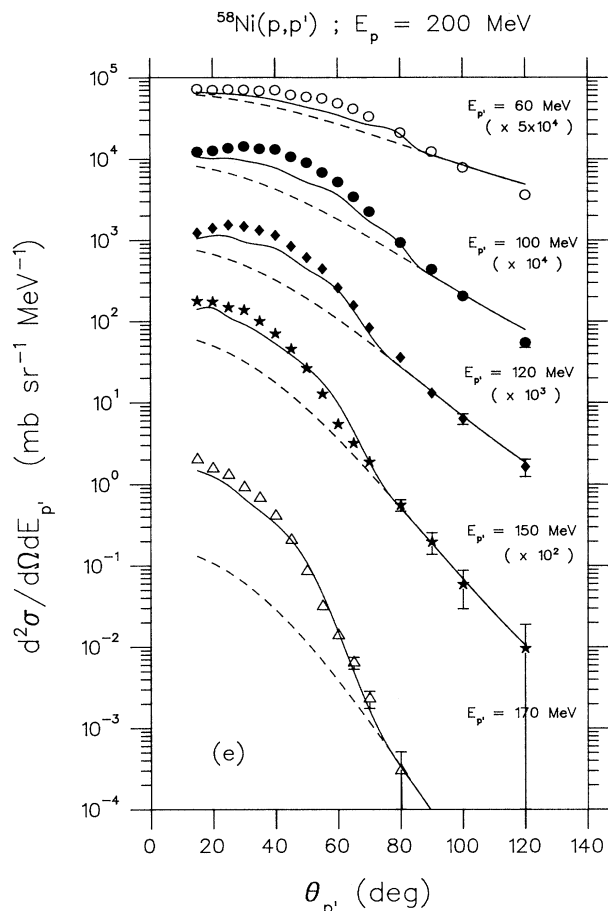


FIG. 3. (Continued).

(DWIA) plus a parametrized multiple-scattering part are also shown in Fig. 3. The overall agreement of the calculated angular distributions with the experimental data is encouraging.

The parametrized angular distribution cross sections were normalized to the experimental data at the most-backward angles where the quasifree component is assumed to be negligible. These normalizations, as reflected in the values of  $\sigma_D$  in Eq. (4), are displayed in Fig. 4. The quantity  $\sigma_D$  is related to the angle-integrated yield, and as a consistency check on these values of  $\sigma_D$ , comparisons have been made with results of calculations with the geometry-dependent hybrid model<sup>36</sup> (GDH). These calculations were performed with the code<sup>37</sup> ALICE. Angle-integrated yields for the reaction  $^{58}\text{Ni}(p,p')$  at 100 and 120 MeV are shown in Fig. 5. Results for  $^{197}\text{Au}(p,p')$  at the same incident energies (derived from Ref. 17) are also shown, and these represent a case which is dominated by the multistep component. (Comparisons at higher incident energies are not expected to be meaningful due to the untested validity of the GDH model at those energies.) The GDH angle-integrated yields in Fig. 5 are qualitatively very similar in shape for  $^{58}\text{Ni}$  and  $^{197}\text{Au}$  at both incident energies. Furthermore, the parametrized calculations for the two targets are also in qualitative shape agreement with each other, and with

the GDH results. From these comparisons it consequently appears that the normalizations of the parametrized angular distributions are reasonable.

A slight preference was developed for the initial-energy prescription (IEP) in the DWIA formalism as this approximation yields somewhat better agreement with the experimental data than the final-energy prescription (FEP) towards lower incident energies. This is in agreement with an investigation of the applicability of the DWIA theory to  $^{12}\text{C}(p,p')$  at 90 and 200 MeV (Ref. 16). The choice of prescription becomes less important with increasing energy, as was also shown in Ref. 16 at 200 MeV. Although no renormalization was necessary in adding the DWIA knockout contributions incoherently from only four (three proton, one neutron) states in  $^{58}\text{Ni}$  to the multistep background, it is probably fortuitous that the neglect of other states is not reflected in a need to adjust this normalization. Furthermore, it is remarkable that the same set of spectroscopic factors of the four states could be used without renormalization for all incident energies, as DWIA fits to coincidence data have often required<sup>38,39</sup> energy-dependent spectroscopic factors.

In order to quantify the proportion which is believed to originate from a quasifree scattering process in the total preequilibrium yield, total integrated cross sections for the quasifree and the parametrized distributions were calculated. The integrations were performed over the solid angle of the observed proton, over an energy range between 20 MeV and that corresponding to an excitation energy of 10 MeV. Thus the region of discrete states, and that of evaporation from an equilibrated nuclear system, are excluded from the integrated yield. The relative

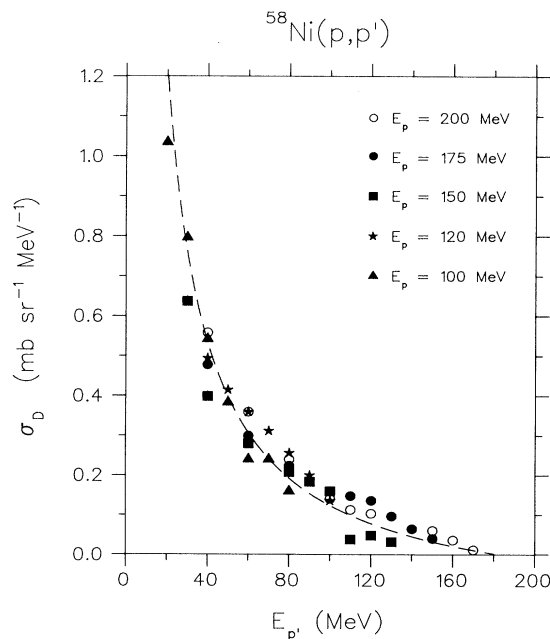


FIG. 4. Normalization factor  $\sigma_D$  as a function of emission energy  $E_{p'}$  for various incident energies  $E_p$ . The dashed curve serves to guide the eye.

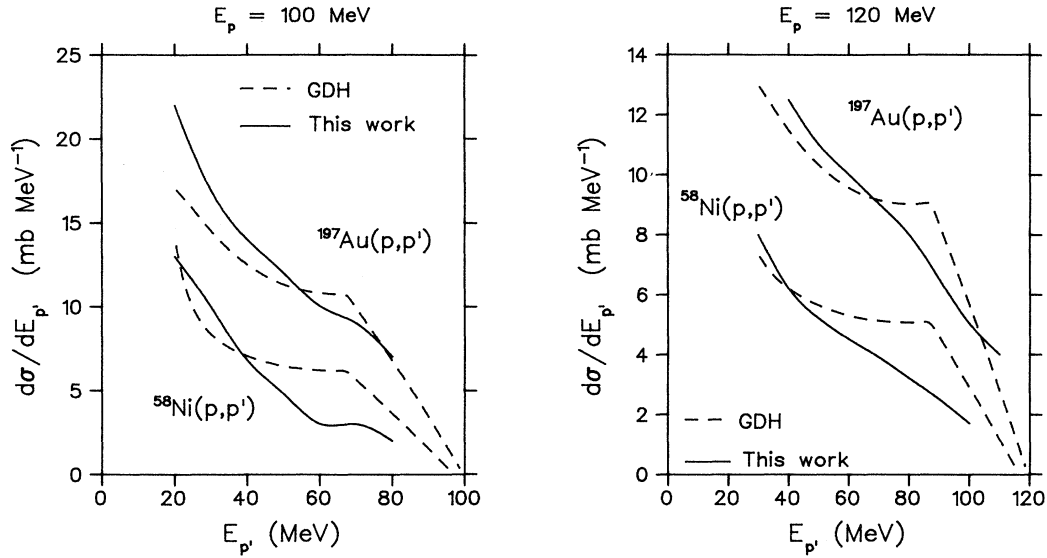


FIG. 5. Comparison between angle-integrated cross sections obtained in this work for the parametrized multiple scattering, and the predictions of the geometry-dependent hybrid (GDH) model.

quasifree contributions in this ejectile energy region are given in Table I. The calculations suggest that  $\sim 30\%$  of the preequilibrium yield from the reaction  $^{58}\text{Ni}(p,p')$  at the various incident energies originates from a single quasifree knockout process. The relative yield of this single knockout contribution is found to be independent of the incident energy, except for an indication of a slight increase from 100 to 120 MeV.

The insensitivity of the quasifree knockout contribution to the preequilibrium yield would at first seem to be inconsistent with general ideas regarding distortion effects in the DWIA. For example, for  $s$ -state knockout on a range of nuclei, Roos<sup>40</sup> finds the ratio of DWIA to plane wave at the maximum of the cross section (which is a measure of the distortion) to increase by roughly an order of magnitude between 100 and 200 MeV bombarding energy. This trend is confirmed experimentally by, e.g., Pugh *et al.*<sup>41</sup> for  $^4\text{He}$ . In our application, however, the angle- and energy-integrated yield is important. Therefore, the fact that increased distortion tends to redistribute the yield in phase space from the plane-wave expectation, causes the integrated cross section to vary much less than suggested by the value of the maximum. In Fig. 6 results for the reaction  $^{58}\text{Ni}(p,2p)^{57}\text{Co}$  are shown for  $2s_{1/2}$  knockout at zero recoil momentum for  $30^\circ$  as one

angle of observation. Also shown is the trend of the secondary-angle integrated cross section (at the primary angle of  $30^\circ$ ) with a value of the observed primary energy which is the same as for the discrete knockout reaction. Although the trivial variation in kinematics has not been removed by dividing by an appropriate plane-wave quantity, the comparison in Fig. 6 illustrates the diminished sensitivity to distortion for the integrated yield.

The single-step component as deduced from the DWIA model is compared in Fig. 7 with the prediction<sup>42</sup> of a statistical multistep-direct (SMD) model based on the

TABLE I. Integrated cross sections for multiple scattering, quasifree scattering, and preequilibrium (MS+QF).

$E_p$ (MeV)	$\sigma_{\text{MS}}$ (mb)	$\sigma_{\text{QF}}$ (mb)	$\sigma_{\text{PE}}$ (mb)	$\sigma_{\text{QF}}/\sigma_{\text{PE}}$
100	360	100	460	0.22
120	400	160	560	0.29
150	380	180	560	0.32
175	440	190	630	0.30
200	490	220	710	0.31

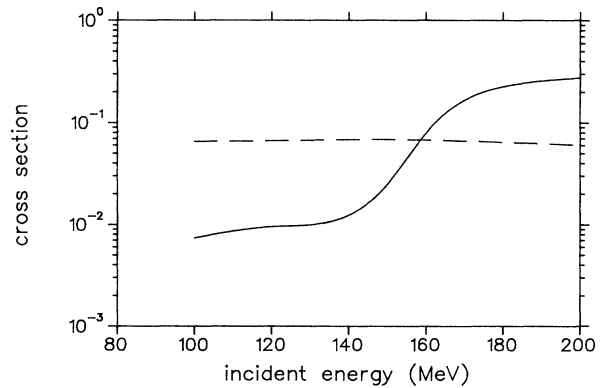


FIG. 6. Incident-energy dependence of  $2s_{1/2}$ -state knockout in the reaction  $^{58}\text{Ni}(p,2p)^{57}\text{Co}$  with  $30^\circ$  as one of the scattering angles. Cross sections for zero recoil momentum (continuous curve in units of  $\text{mb sr}^{-2} \text{MeV}^{-1}$ ), and angle-integrated quantities (dashed curve in units of  $\text{mb sr}^{-1} \text{MeV}^{-1}$ ), at the same momentum transfer, are shown. The numerical scale applies to both curves.



theory of Feshbach, Kerman, and Koonin.<sup>24</sup> The single-scattering yields from the quasifree model are in reasonably good quantitative and qualitative agreement with the results of the SMD model. It is interesting that these two very different approaches to the estimation of the first-step contribution yield such similar results. Although the observed similarity is not studied further in this work, it needs to be investigated by comparing these results with predictions of one-step models, such as that of Luo and Kawai.<sup>43</sup>

Experimental energy spectra, with the multiple-scattering contribution subtracted, are shown in Fig. 8. These are for an incident energy of 200 MeV, i.e., the spectra of Fig. 2(e) with the MS contribution from Fig. 3(e). We find that the spectra in Fig. 8 manifest prominent quasifree peaks, as opposed to the original data.

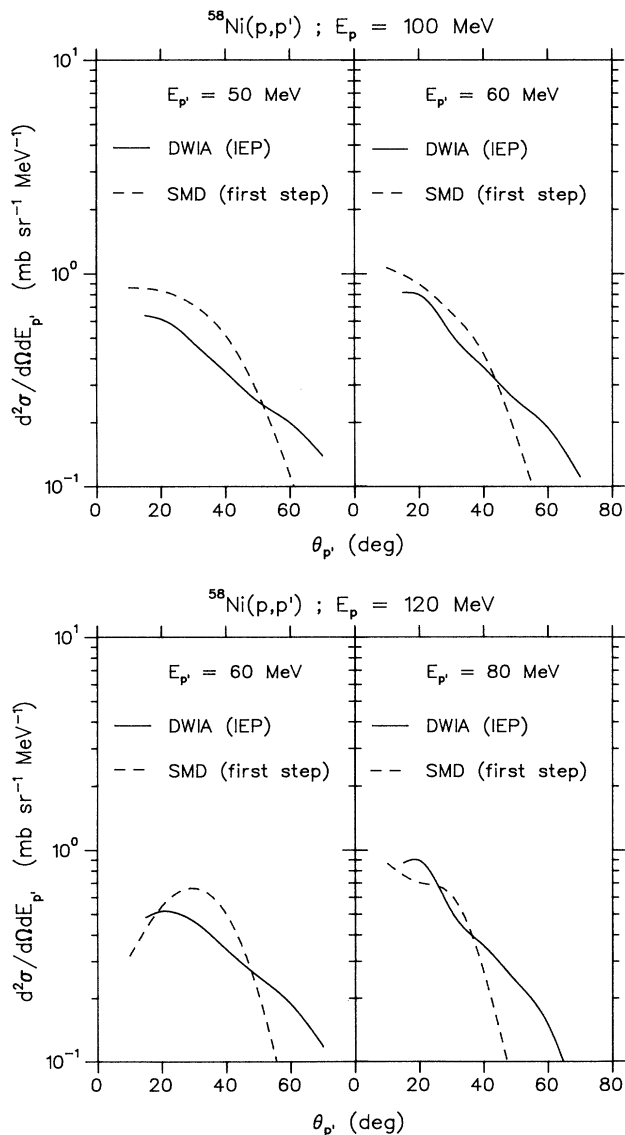


FIG. 7. Comparison between DWIA calculations of this work and first-step SMD predictions of Ref. 42.

The observed agreement between the theoretical results and the experimental angular distributions is satisfactory if one considers the simplicity of the calculations. This study suggests the importance of an initial nucleon-nucleon interaction, in spite of a large background of multiple scattering which obscures the single-step signature to a large extent. Consequently, quasifree knockout appears to be an important component of the reaction mechanism leading to protons scattering into the continuum.

## VI. SUMMARY AND CONCLUSIONS

Continuum spectra for the inclusive reaction  $^{58}\text{Ni}(p,p')$  were measured at incident energies of 100, 120, 150, 175, and 200 MeV at scattering angles between  $15^\circ$  and  $120^\circ$ . Angular distributions for various ejectile energies were interpreted in terms of a model which considers a quasifree knockout component which is added incoherently to

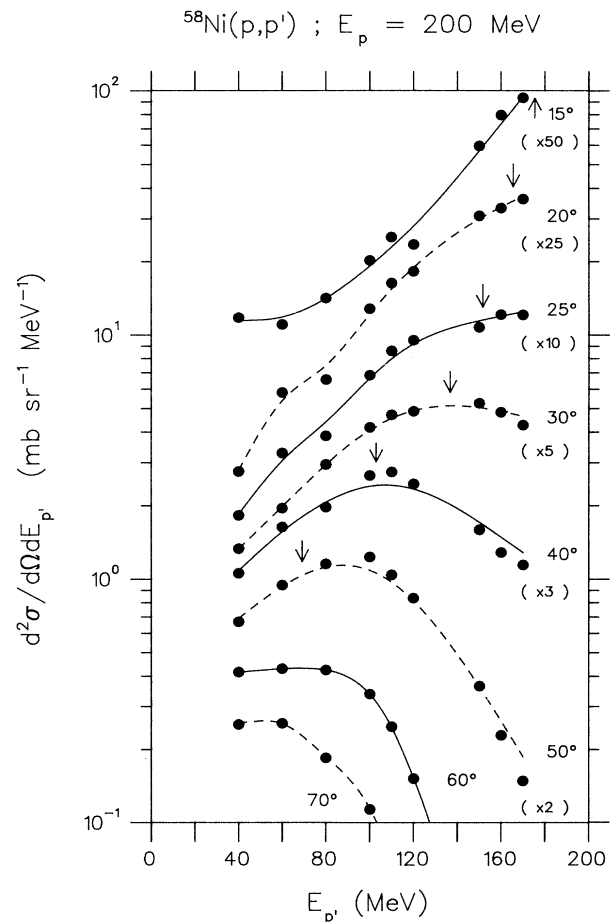


FIG. 8. Experimental energy spectra, with the inferred multiple-scattering component subtracted, at an incident energy of 200 MeV as a function of emission energy  $E_{p'}$ . The expected locations of quasifree scattering peaks for the kinematics of interaction with a target nucleon bound by  $\sim 10$  MeV are indicated by arrows.

a multistep contribution derived from a phenomenological parametrization. A consistent calculation gives agreement with the experimental data over the range of incident energies which was explored.

The proportion of quasifree scattering is found to be  $\sim 30\%$  of the preequilibrium yield over the entire range of incident energies, and this value is much less than that implied by the work of Smith and Bozoian,<sup>5</sup> but much larger than the value adopted by Kalbach.<sup>15</sup> On the oth-

er hand, the amount of quasifree scattering is in excellent agreement with the first-step contribution predicted by the statistical multistep-direct model.

We have shown that preequilibrium spectra can be successfully analyzed in terms of a simple quasifree knockout model added to a phenomenological parametrization of the multistep component. Clearly, extension of this application to other target masses, and to higher incident energies, is desirable.

- <sup>1</sup>H. Machner, Phys. Rep. **127**, 309 (1985).  
<sup>2</sup>H. Gruppelaar, P. Nagel, and P. E. Hodgson, Riv. Nuovo Cimento **9**, 1 (1986).  
<sup>3</sup>J. R. Wu, Phys. Lett. **91B**, 169 (1980).  
<sup>4</sup>H. C. Chiang and J. Hüfner, Nucl. Phys. **A349**, 466 (1980).  
<sup>5</sup>R. D. Smith and M. Bozoian, Phys. Rev. C **39**, 1751 (1989).  
<sup>6</sup>N. S. Wall and P. R. Roos, Phys. Rev. **150**, 811 (1966).  
<sup>7</sup>H. Machner, D. Protić, G. Riepe, J. P. Didelez, N. Frascaria, E. Gerlic, E. Hourani, and M. Morlet, Phys. Lett. **138B**, 39 (1984).  
<sup>8</sup>R. E. Segel, S. M. Levenson, P. Zupranski, A. A. Hassan, S. Mukhopadhyay, and J. V. Maher, Phys. Rev. C **32**, 721 (1985).  
<sup>9</sup>R. E. Chrien, T. J. Krieger, R. J. Sutter, M. May, H. Palevsky, R. L. Stearns, T. Kozlowski, and T. Bauer, Phys. Rev. C **21**, 1014 (1980).  
<sup>10</sup>J. R. Wu, C. C. Chang, and H. D. Holmgren, Phys. Rev. C **19**, 698 (1979).  
<sup>11</sup>T. Chen, R. E. Segel, P. T. Debevec, John Wiggins, P. P. Singh, and J. V. Maher, Phys. Lett. **103B**, 192 (1981).  
<sup>12</sup>F. E. Bertrand, W. R. Burrus, N. W. Hill, T. A. Love, and R. W. Peelle, Nucl. Instrum. and Methods **101**, 475 (1972).  
<sup>13</sup>A. A. Cowley, C. C. Chang, and H. D. Holmgren, Phys. Rev. C **22**, 2633 (1980).  
<sup>14</sup>C. Kalbach, Phys. Rev. C **37**, 2350 (1988).  
<sup>15</sup>C. Kalbach, Phys. Rev. C **41**, 1656 (1990).  
<sup>16</sup>S. V. Förtisch, A. A. Cowley, J. V. Pilcher, D. M. Whittal, J. J. Lawrie, J. C. van Staden, and E. Friedland, Nucl. Phys. **A485**, 258 (1988).  
<sup>17</sup>A. A. Cowley, S. V. Förtisch, J. J. Lawrie, D. M. Whittal, F. D. Smit, and J. V. Pilcher, Z. Phys. A **336**, 189 (1990).  
<sup>18</sup>A. A. Cowley, S. V. Förtisch, J. J. Lawrie, J. V. Pilcher, F. D. Smit, and D. M. Whittal, Europhys. Lett. **13**, 37 (1990).  
<sup>19</sup>D. M. Whittal, A. A. Cowley, J. V. Pilcher, S. V. Förtisch, F. D. Smit, and J. J. Lawrie, Phys. Rev. C **42**, 309 (1990).  
<sup>20</sup>N. S. Chant and P. G. Roos, Phys. Rev. C **15**, 57 (1977); P. Kitching, W. J. McDonald, Th. A. J. Maris, and C. A. Z. Vasconcellos, in *Advances in Nuclear Physics*, edited by J. W. Negele and Erich Vogt (Plenum, New York, 1985), Vol. 15, p. 43.  
<sup>21</sup>J. S. Wesick, P. G. Roos, N. S. Chant, C. C. Chang, A. Nadasen, L. Rees, N. R. Yoder, A. A. Cowley, S. J. Mills, and W. W. Jacobs, Phys. Rev. C **32**, 1474 (1985).  
<sup>22</sup>J. V. Pilcher, A. A. Cowley, D. M. Whittal, and J. J. Lawrie, Phys. Rev. C **40**, 1937 (1989).  
<sup>23</sup>R. E. L. Green, D. H. Boal, R. L. Helmer, K. P. Jackson, and R. G. Korteling, Nucl. Phys. **A405**, 463 (1983).  
<sup>24</sup>Herman Feshbach, Arthur Kerman, and Steven Koonin, Ann. Phys. (N.Y.) **125**, 429 (1980).  
<sup>25</sup>N. S. Chant, code THREEDDEE, University of Maryland (unpublished).  
<sup>26</sup>G. Ciangaru, C. C. Chang, H. D. Holmgren, A. Nadasen, and P. G. Roos, Phys. Rev. C **29**, 1289 (1984).  
<sup>27</sup>A. Nadasen, P. Schwandt, P. P. Singh, W. W. Jacobs, A. D. Bacher, P. T. Debevec, M. D. Kaitchuck, and J. T. Meek, Phys. Rev. C **23**, 1023 (1981).  
<sup>28</sup>Edward F. Redish, G. J. Stephenson, Jr., and Gerald M. Lerner, Phys. Rev. C **2**, 1665 (1970).  
<sup>29</sup>Gerhard Jacob and Th. A. J. Maris, Rev. Mod. Phys. **38**, 121 (1966); **45**, 6 (1973).  
<sup>30</sup>N. S. Chant, P. Kitching, P. G. Roos, and L. Antonuk, Phys. Rev. Lett. **43**, 495 (1979).  
<sup>31</sup>G. Jacob, Th. A. J. Maris, C. Schneider, and M. R. Teodoro, Phys. Lett. **45B**, 181 (1973); Gerhard Jacob, Th. A. J. Maris, C. Schneider, and M. R. Teodoro, Nucl. Phys. **A257**, 517 (1976).  
<sup>32</sup>F. Perey and B. Buck, Nucl. Phys. **32**, 353 (1962).  
<sup>33</sup>K. Reiner, P. Grabmayr, G. J. Wagner, S. M. Banks, B. G. Lay, V. C. Officer, G. G. Shute, B. M. Spicer, C. W. Glover, W. P. Jones, D. W. Miller, H. Nann, and E. J. Stephenson, Nucl. Phys. **A472**, 1 (1987).  
<sup>34</sup>W. Scobel, M. Trabandt, M. Blann, B. A. Pohl, B. R. Remington, R. C. Byrd, C. C. Foster, R. Bonetti, C. Chiesa, and S. M. Grimes, Phys. Rev. C **41**, 2010 (1990).  
<sup>35</sup>A. A. Cowley, A. van Kent, J. J. Lawrie, S. V. Förtisch, D. M. Whittal, J. V. Pilcher, F. D. Smit, W. A. Richter, R. Lindsay, I. J. van Heerden, R. Bonetti, and P. E. Hodgson, Phys. Rev. C **43**, 678 (1990).  
<sup>36</sup>M. Blann and H. K. Vonach, Phys. Rev. C **28**, 1475 (1983).  
<sup>37</sup>M. Blann, code ALICE/85/300, Lawrence Livermore National Laboratory Report UCID-20169, 1984 (unpublished).  
<sup>38</sup>C. Samanta, N. S. Chant, P. G. Roos, A. Nadasen, J. Wesick, and A. A. Cowley, Phys. Rev. C **34**, 1610 (1986).  
<sup>39</sup>P. Kitching, C. A. Miller, D. A. Hutcheon, A. N. James, W. J. McDonald, J. M. Cameron, W. C. Olsen, and G. Roy, Phys. Rev. Lett. **37**, 1600 (1976).  
<sup>40</sup>P. G. Roos, in *Momentum Wave functions—1976*, Proceedings of the Workshop/Seminar on Momentum Wave Function Determination in Atomic, Molecular, and Nuclear Systems, edited by D. W. Devins, AIP. Conf. Proc. No. 36 (AIP, New York, 1977), p. 32.  
<sup>41</sup>H. G. Pugh, P. G. Roos, A. A. Cowley, V. K. C. Cheng, and R. Woody, Phys. Lett. **46B**, 192 (1973).  
<sup>42</sup>W. A. Richter (private communication).  
<sup>43</sup>Y. L. Luo and M. Kawai, Phys. Lett. B **235**, 211 (1990).